

## MIT Open Access Articles

### *Contrail coverage over the United States before and during the COVID-19 pandemic*

The MIT Faculty has made this article openly available. **Please share** how this access benefits you. Your story matters.

**Citation:** Meijer, Vincent R, Kulik, Luke, Eastham, Sebastian D, Allroggen, Florian, Speth, Raymond L et al. 2022. "Contrail coverage over the United States before and during the COVID-19 pandemic." *Environmental Research Letters*, 17 (3).

**As Published:** 10.1088/1748-9326/AC26F0

**Publisher:** IOP Publishing

**Persistent URL:** <https://hdl.handle.net/1721.1/145277>

**Version:** Final published version: final published article, as it appeared in a journal, conference proceedings, or other formally published context

**Terms of use:** Creative Commons Attribution 4.0 International license



LETTER • **OPEN ACCESS**

## Contrail coverage over the United States before and during the COVID-19 pandemic

To cite this article: Vincent R Meijer *et al* 2022 *Environ. Res. Lett.* **17** 034039

View the [article online](#) for updates and enhancements.

You may also like

- [Preface](#)

- [Preface](#)

- [Preface](#)

ENVIRONMENTAL RESEARCH  
LETTERS

## LETTER




## Contrail coverage over the United States before and during the COVID-19 pandemic

## OPEN ACCESS

RECEIVED  
21 May 2021REVISED  
23 July 2021ACCEPTED FOR PUBLICATION  
15 September 2021PUBLISHED  
7 March 2022

Original content from  
this work may be used  
under the terms of the  
[Creative Commons  
Attribution 4.0 licence](#).

Any further distribution  
of this work must  
maintain attribution to  
the author(s) and the title  
of the work, journal  
citation and DOI.

Vincent R Meijer<sup>1,4</sup>, Luke Kulik<sup>1,4</sup>, Sebastian D Eastham<sup>1,2</sup> , Florian Allroggen<sup>1,2</sup>, Raymond L Speth<sup>1,2</sup> ,  
Sertac Karaman<sup>3</sup> and Steven R H Barrett<sup>1,2,\*</sup> <sup>1</sup> Laboratory for Aviation and the Environment, Department of Aeronautics and Astronautics, Massachusetts Institute of Technology, Cambridge, MA, 02139, United States of America<sup>2</sup> Joint Program on the Science and Policy of Global Change, Massachusetts Institute of Technology, Cambridge, MA, 02139, United States of America<sup>3</sup> Laboratory for Information and Decision Systems, and Department of Aeronautics and Astronautics, Massachusetts Institute of Technology, Cambridge, MA, 02139, United States of America<sup>4</sup> Co-first authors

\* Author to whom any correspondence should be addressed.

E-mail: [sbarrett@mit.edu](mailto:sbarrett@mit.edu)**Keywords:** contrails, aviation, remote sensing, COVIDSupplementary material for this article is available [online](#)**Abstract**

Contrails are potentially the largest contributor to aviation-attributable climate change, but estimates of their coverage are highly uncertain. No study has provided observation-based continental-scale estimates of the diurnal, seasonal, and regional variability in contrail coverage. We present contrail coverage estimates for the years 2018, 2019 and 2020 for the contiguous United States, derived by developing and applying a deep learning algorithm to over 100 000 satellite images. We estimate that contrails covered an area the size of Massachusetts and Connecticut combined in the years 2018 and 2019. Comparing 2019 and 2020, we quantify a 35.8% reduction in distance flown above 8 km altitude and an associated reduction in contrail coverage of 22.3%. We also find that the diurnal pattern in contrail coverage aligns with that of flight traffic, but that the amount of contrail coverage per distance flown decreases in the afternoon.

Condensation trails, or contrails, are ice clouds that form as a result of the mixing of cold, humid air with aircraft engine exhaust plumes [1]. They affect the radiative balance of Earth by increasing global cloudiness, interacting both with incoming solar and outgoing thermal radiation [2]. Contrails have been shown to result in net positive radiative forcing (RF), thereby contributing to climate change [3]. Studies find that contrails and contrail cirrus may be the largest contributor to aviation-attributable RF [2], potentially exceeding contributions of aviation CO<sub>2</sub> emissions. This means that contrails associated with today's flight activity may result in as much instantaneous warming as the entire atmospheric stock of aviation-attributable CO<sub>2</sub> that has accumulated since the beginning of the jet age. Because reductions in contrail RF could be achieved quickly and could halve aviation-attributable warming, contrail avoidance strategies have been widely investigated [4–6]. Successful implementation of such strategies

requires improved capabilities for observing contrails and contrail cirrus, and empirically quantifying their impact and relation to flights. In particular, the diurnal cycle of contrail formation and persistence has not previously been accurately quantified, but will affect the net climate impacts of individual flights.

Most estimates of contrail properties and climate impacts have relied on atmospheric modelling [7–9]. Observational data on contrails can help the validation of these models and potentially reduce the uncertainty in estimates of overall RF from contrails, which currently vary by an order of magnitude [2, 10]. Several studies have quantified contrail coverage and impacts using data from satellites in low earth orbit (LEO) [3, 11–15]. Since these satellites are typically constrained to two overpasses per day, LEO-based observations of contrails are less suited to gather information on diurnal variations. This is of particular relevance to contrails, where the likelihood of formation and the overall impacts vary significantly

between times of day. To obtain more than one nighttime and one daytime image from LEO-based observations requires combining data from multiple satellites, as in prior work by Duda *et al* [15]. On the other hand, geostationary satellites can provide continuous observations at large scale, but contrail detection on images from these satellites is difficult due to the coarser spatial resolution. Whereas many LEO satellite imagers feature pixel sizes of 1 km or less, imagers on geostationary satellites with small-footprint pixels (e.g. 2 km) for infrared bands have only recently become available. This is important for automated contrail detection because the average width for most contrails is 4–6 km and individual contrails can be much narrower, making them difficult to detect in geostationary imagery [13]. Prior to this work, the only automated analyses of contrails on geostationary satellite imagery have involved tracking a small number of contrails which were first identified using LEO imaging [16–18], a case study of contrail clusters over the Great Lakes [19], and application of a contrail classification network to three months of Advanced Himawari Imager data [20]. As such, this study is the first to apply an automated contrail detection algorithm which operates at a pixel-by-pixel level to multiple years of geostationary satellite data.

In this work we present the results of the first automated contrail detection algorithm working with geostationary satellite imagery from the Advanced Baseline Imager (ABI) [21] aboard the Geostationary Operational Environmental Satellite 16 (GOES-16). The detection algorithm is a convolutional neural network that is trained with a dataset of 103 manually labelled GOES-16 ABI-L2-MCMIPF [22] images that cover the contiguous United States, and therefore the majority of air traffic in the satellite's field of view. We estimate contrail coverage from approximately 100 000 satellite images, amounting to nearly six trillion pixels, for the period 1 January 2018 to 31 December 2020. This includes the period of unprecedented reduction in aircraft traffic due to the COVID-19 pandemic. A single image is made up of six million pixels, with each pixel representing an area of approximately 2 by 2 km.

The dataset containing manual labels of contrails was produced by individuals trained to interpret remote sensing data. The labellers made use of the Ash RGB product, a false colour composite that combines four of the GOES-16 ABI infrared bands, in order to improve their ability to distinguish between clouds. Contrails tend to occupy significantly smaller portions of the image than natural clouds and are typically only a few pixels wide, making the manual identification and labelling of contrails a costly and difficult task. Contrails were primarily identified by looking for line-shaped thin cirrus clouds, but natural cirrus clouds may also exhibit such linear patterns and are therefore a potential source of incorrectly labelled contrails. Both contrails in clear sky and

embedded within cirrus clouds have been labelled. In order to avoid mis-labelling natural cirrus as contrails we presented labellers with a sequence of images of the 2 h leading up to the image to be labelled. This allowed the labellers to distinguish between natural cirrus and contrails, since contrails first appear with a linear shape and slowly deform as they age, whereas natural cirrus often shows the opposite behaviour where linear shapes evolve as they age under the influence of local wind patterns. Further details on the labelling procedure, including examples and validation procedures, are given in the methods section and supplementary information (available online at [stacks.iop.org/ERL/17/034039/mmedia](https://stacks.iop.org/ERL/17/034039/mmedia)).

We evaluate the performance of the contrail detection algorithm on a test set of 19 manually labelled images which have not been used while training the algorithm. Averaged over this test set, the precision and recall are 52.5% and 50.2%, respectively, indicating a balance between over- and under-prediction by the network. Both of these metrics are in terms of the number of pixels. When quantifying precision and recall in terms of connected components, we obtain a precision of 51.7% and a recall of 71.3%. Precision and recall are quantified by both season and time of day in extended figure 5.

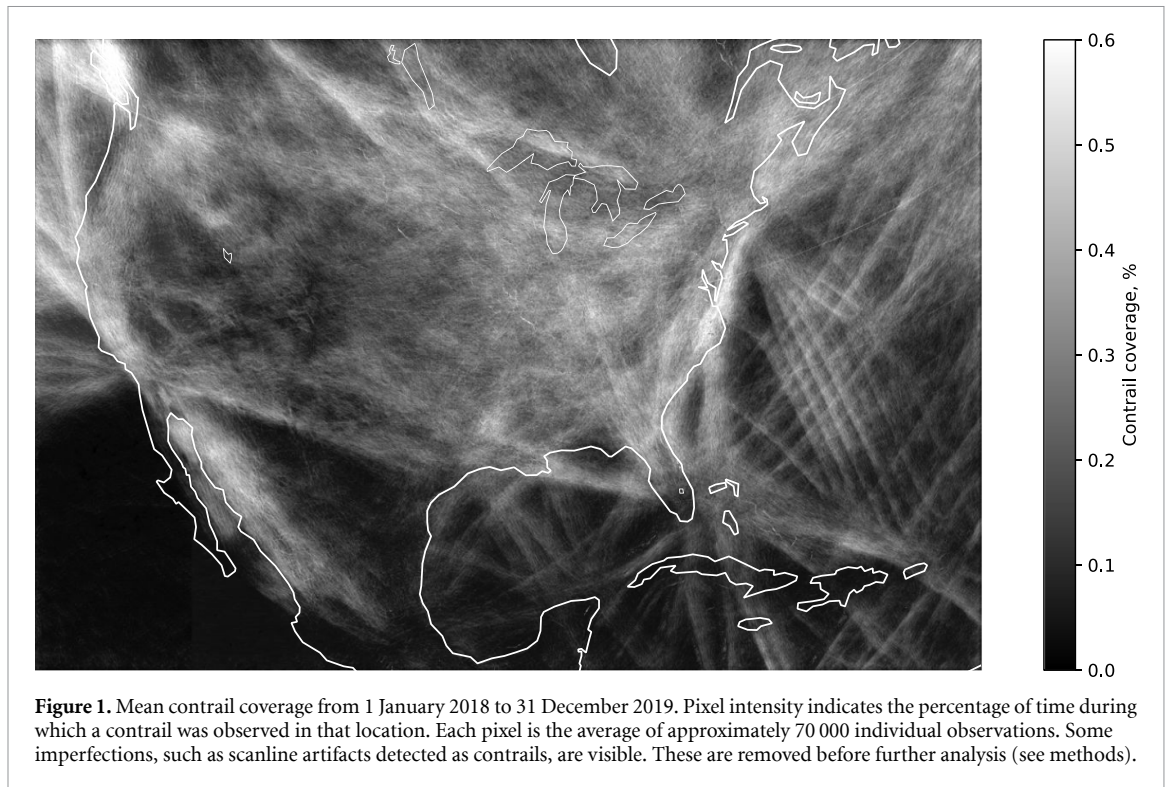
Both these performance metrics are comparable to those of other contrail detection algorithms which used higher-resolution LEO satellite data [11–13]. In terms of contrail coverage, our average error on the test set is 0.0146%. Examples of our algorithm's performance on the testing set are given in the supplementary materials.

Once trained, we use our algorithm to estimate contrail coverage every 10–15 min from 1 January 2018 to 31 December 2020, resulting in over 0.8 trillion pixel-wise estimates of contrail coverage for the contiguous US as well as parts of Canada, Mexico, the Caribbean and the Pacific and Atlantic oceans. We also use flight traffic data [23] derived from ADS-B measurements to study the relationship between contrail coverage and flight. In each image, each of the six million pixels are classified as either 'contrail' or 'not contrail' before the contrail-covered area is calculated. Further details on the computation of contrail coverage from the algorithm output can be found in the methods section.

## 1. Results

### 1.1. Contrail coverage over the contiguous United States

Figure 1 shows our estimated average contrail coverage for 2018–2019. Major flight corridors (e.g. off the East Coast of the US and along transcontinental routes) and 'holes' in coverage at major airports as aircraft descend below contrail forming regions (e.g. Miami) are visible. Averaged over 2018 and 2019, we find that 0.17% of the domain was covered by



contrails. At 43 000 km<sup>2</sup> this is an area similar in size to Massachusetts and Connecticut combined. When limited to airspace over the contiguous US, average contrail coverage is 0.26%. When we consider the airspace over the oceans in the domain, we find that on average 0.15% is covered with contrails. These estimates of contrail coverage are lower than those reported in other studies, but direct comparison with previous estimates is complicated by several factors. To date, estimates of contrail coverage are exclusively based on either models or detections on LEO satellite imagery: no estimate of contrail coverage has been based on imagery at the 10–15 min resolution we use here. We are therefore able to average over the entire day instead of a handful of overpass times, as was the case for previous satellite-based studies. One such study by Palikonda *et al* [12], also focusing on the continental United States, found a 1.29% and 0.71% average coverage for morning (7:30 local time) and afternoon (14:30 local time) overpasses respectively. Part of the discrepancy between these numbers and the ones found here may be explained by the overpass times of the LEO satellites. For example, if we take the average of two years of contrail detections as observed between 10 and 11 am local solar time (relevant to a sun-synchronous satellite), we find a coverage fraction 57% greater than the ‘true’ mean value (considering only the six areas shown in figure 2). Depending on the overpass time, this discrepancy varies from –52% to +90%, illustrating how overpass time can affect estimates of contrail coverage. If we consider the average contrail coverage for a day-time (10–11:00 local time) and night-time (22–23:00

local time) overpass window, as was done in previous studies [13, 15], we find a smaller deviation from the mean value of 18%. This confirms that combining contrail observations from LEO satellite overpasses from different times can lead to less biased estimates of the true average. Other differences with previous satellite-based estimates may be attributed to the coarser spatial resolution of the instrument used in this study, which inherently limits the number of contrails visible on the relevant images. Based on statistics of contrail width reported by Duda *et al* [13], we estimate that between 10.2% and 12.2% of contrails detected on 1 km resolution imagery have widths less than 2 km. The numbers presented here are therefore a lower bound on contrail coverage.

At longer timescales, we find that the standard deviation of the weekly-average distance flown is 51%, whereas that of contrail coverage is 60.7%. These statistics ignore the spatial distribution, and its variation, of distance flown and contrail coverage, such that the actual contribution of weather to the weekly changes is likely to be larger than these numbers suggest. We also find that contrail coverage peaks near the end of winter and start of the spring with values of 0.35%–0.4%, and reaches its lowest values of 0.05%–0.1% in summer and early fall. Similar seasonal and weekly variations in contrail coverage have been found in previous studies [11–13, 24, 25]. In order to illustrate the day-to-day variation of contrail coverage and its relation to the synoptic meteorological conditions, we present a comparison of the 500 hPa geopotential height and observed contrail

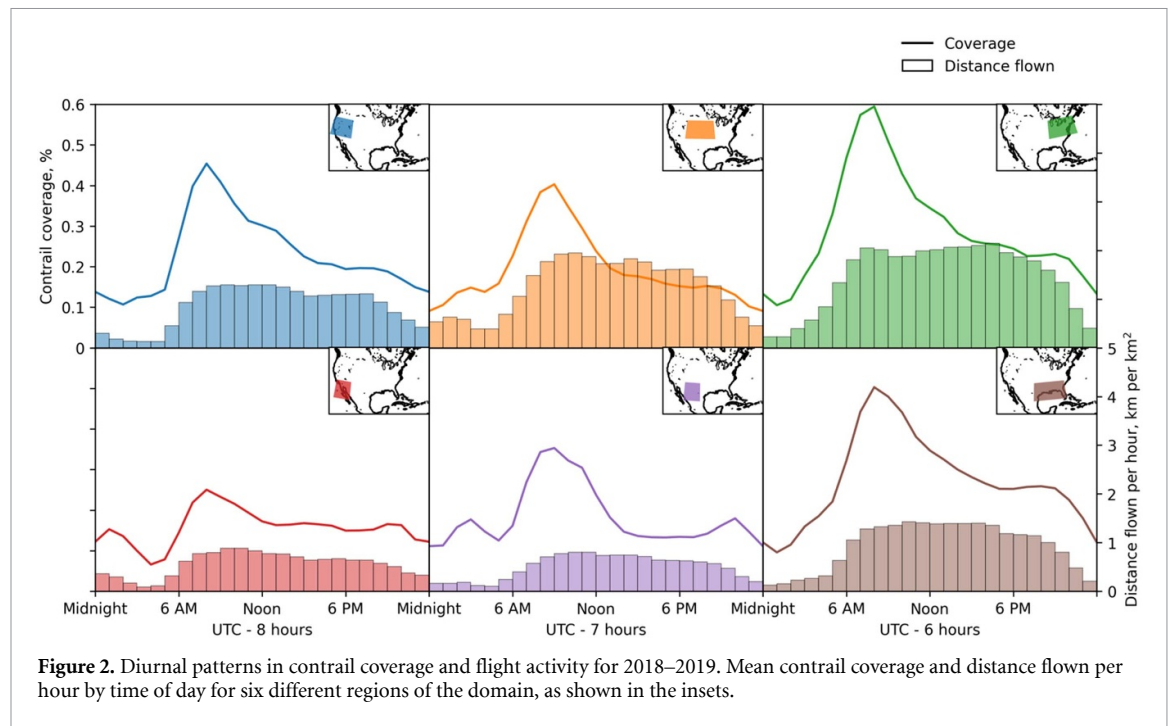


**Figure 2.** Diurnal patterns in contrail coverage and flight activity for 2018–2019. Mean contrail coverage and distance flown per hour by time of day for six different regions of the domain, as shown in the insets.

coverage for a sequence of four days in extended figure 6.

### 1.2. Diurnal patterns in contrail coverage and distance flown

In figure 2 we show the diurnal variation in both contrail coverage and flight traffic in six different regions of the US as a function of local time. For all six regions, contrail coverage peaks between 08:00 and 09:00 at values between 0.31% (southwest) and 0.60% (northwest). Surface-based observations in the US have also reported the frequency of contrail occurrence to peak in mid-morning [24]. Contrail coverage is minimized between 00:00 and 05:00 at values between 0.084% (southwest) and 0.11% (northeast). The resulting diurnal variations in contrail coverage are between a factor of 3.3 (south central) and 5.2 (northeast). Overlaid on figure 2 we show the average diurnal pattern of flight activity based on transponder data. We find that distance flown peaks one to three hours later between 09:00 and 11:00 local time in all regions but the Northeast. Whereas contrail coverage in all regions declines from its morning peak value, distance flown remains approximately constant up until the evening. A study by Palikonda *et al* [12], covering a similar domain, also found a near halving of contrail coverage between 7:30 and 14:30 local time. This may suggest that the sensitivity of contrail coverage to flight activity is greatest at night and in the early morning ( $141 \text{ m}^2$  of cover per meter flown between 6 am and noon), and is lowest in the afternoon and early evening ( $85.2 \text{ m}^2 \text{ m}^{-1}$  between noon and 6 pm).

An alternative explanation could be a reduction in detection efficiency of the algorithm in the afternoon,

but the validation of our algorithm's performance against manually labelled images does not corroborate this (see extended figure 5). However, it is also possible that contrails are less recognizable in the afternoon, both by means of manual and automated identification. This may be the case if they were to form within or below existing cirrus clouds which have been observed to peak in coverage in the afternoon [26]. Minnis *et al* [27] suggested that spreading of contrails formed during the morning could lead to less visually distinct contrails forming in the afternoon as they occur in a pre-existing cirrus cloud of artificial origin. This may contribute to the perceived reduction in contrail coverage during the afternoon, in both the human-labelled and automatically-labelled images. Further study is needed to explain this behaviour, possibly involving additional sources of observations and models.

We also find seasonal variations in contrail coverage, independent of traffic volumes. Coverage per unit distance flown is at its greatest during winter and spring ( $293$  and  $296 \text{ m}^2 \text{ m}^{-1}$ ), and at its lowest in summer ( $138 \text{ m}^2 \text{ m}^{-1}$ ). This is consistent with prior studies of observed contrail coverage [12, 19].

### 1.3. The impact of COVID-19 on contrail coverage

In figure 3 we show contrail coverage as a function of time for three full years, namely 2018, 2019 and 2020. This includes the unprecedented long-term reduction in worldwide flight activity during the COVID-19 pandemic, which we show here by plotting the distance flown above 8 km pressure altitude in the analysis domain (dashed line). The most significant flight activity reduction occurs at the end of March, after which it slowly increases. In the month of April,

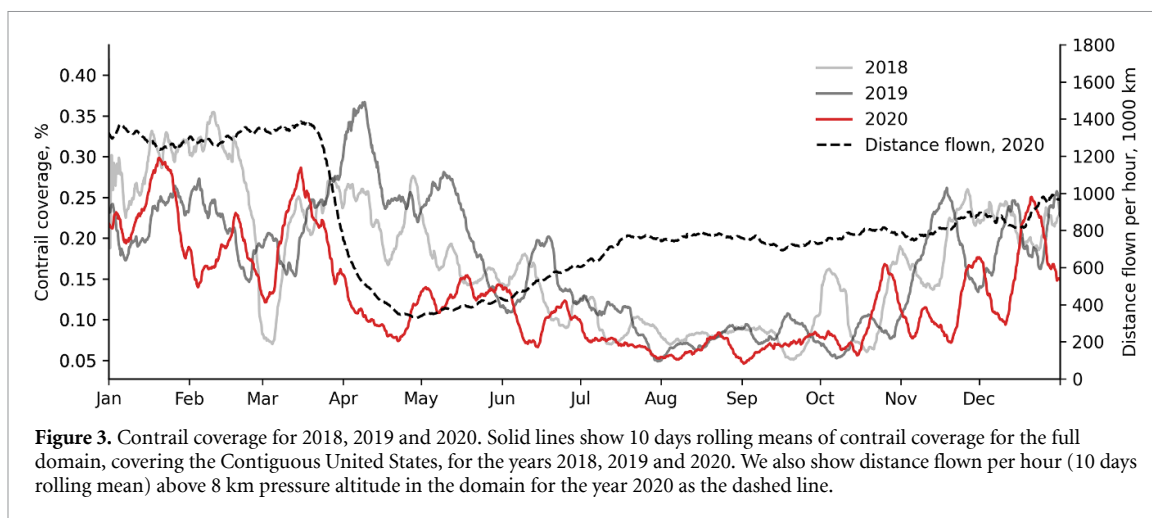


**Figure 3.** Contrail coverage for 2018, 2019 and 2020. Solid lines show 10 days rolling means of contrail coverage for the full domain, covering the Contiguous United States, for the years 2018, 2019 and 2020. We also show distance flown per hour (10 days rolling mean) above 8 km pressure altitude in the domain for the year 2020 as the dashed line.

flight distance is on average 65.3% (95% CI: 63.5%, 67.0%) lower than in the month of March, accompanied by a relative reduction of 48.7% in observed contrail coverage. Other studies have also found reductions in cirrus coverage, which contrail coverage is a part of, for these periods and correlate the changes with those in air traffic [28, 29]. When comparing the year 2020 to the aggregate of 2018 and 2019, we find a reduction of 24.1% (95% CI: 23.3%, 24.9%) in average contrail coverage. When directly comparing 2019 and 2020, the reduction is 22.3% (95% CI: 21.4%, 23.2%). This is less than the change in distance flown, which reduced by 35.8% (95% CI: 35.3%, 36.5%) in 2020 compared to 2019. For comparison, month-to-month variation in the total distance flown by US domestic carriers in 2018 and 2019 was less than  $\pm 10\%$ , based on data from the US Bureau of Transportation Statistics [30].

Some insight into the cause of this discrepancy can be gained by comparing the non-COVID years of 2018 and 2019. Distance flown in the target domain increased by 5% from 2018 to 2019, while contrail coverage instead fell by 5.4% (95% CI: 4.3%, 6.5%), similar to the differences found between 2006 and 2012 by Duda *et al* [15]. This difference is similar in magnitude to the discrepancy between the reduction in distance flown during 2020 and the reduction in contrail coverage, and demonstrates the possibility of a non-linear relationship between flight distance and contrail coverage which is subject to inter-annual (meteorological) variability. This is further corroborated by recent modelling studies addressing the contrail changes induced by COVID-19 related air traffic reductions [31, 32].

## 2. Discussion

We use machine learning and geostationary satellite imagery to provide the first continuous, kilometre-scale estimate of contrail coverage, enabling us to quantify the relationship between flight traffic and

contrails at sub-hourly temporal resolution. The large volume of analysed data illustrates the significant day-to-day variability in contrail coverage, but also allows us to extract several insights by performing long-term averaging. For example, the averaged spatial distribution of contrail coverage shows the predominant air traffic corridors, reproducing patterns such as the parallel flight tracks running south-east from airports in New England. Our observations, spanning three full years, have also allowed us to quantify the impact of the air traffic reductions associated with the COVID-19 pandemic on contrail coverage.

Our results suggest a non-linear relationship between contrail coverage and distance flown, with significant influence from meteorological variability. Contrail coverage in 2019 was 5.4% lower than in 2018, in spite of a 5% increase in air traffic (as measured by the distance flown). Our results also show that contrail coverage in all US regions peaks in the local morning and declines by 30%–50% in the afternoon, while distance flown remains almost constant over the same period. An alternative explanation of this phenomenon would be that both manual and automated identification of contrails on satellite images is limited in the afternoon, possibly by increased natural cirrus coverage. We also observe non-linearity between distance flown and contrail coverage when comparing 2019 and 2020. We find that contrail coverage decreased by 22.3% from 2019 to 2020, whereas distance flown at altitudes above 8 km decreased by 35.8%.

Further research is needed to determine the exact origin of the discrepancies between distance flown and observed contrail coverage, both in terms of diurnal patterns and long-term changes such as those associated with the COVID-19 pandemic. These discrepancies may substantively change not only estimates of the climate impacts resulting from aviation, but also how those impacts might be meaningfully reduced.

## Data availability statement

The data that support the findings of this study are available upon reasonable request from the authors.

## Acknowledgments

We would like to thank Dr Martin Schäfer from the University of Oxford for granting us access to the OpenSky database archive, Labelbox for providing us with a platform to label our data, Dr Fangchang Ma (now at Apple) for his insightful discussions during his time at MIT, Nvidia for donating a Quadro P6000 GPU for this work and Amazon Web Services for donating computational resources for this work. This publication was partially supported by NASA research grant 80NSSC19K0943 and the MIT Environmental Solutions Initiative.

## Author contributions

S R H B and S K conceived the project. V R M created the deep learning algorithm and analysed its results. L K led acquisition of the labelled contrails dataset and developed the first version of the algorithm. R L S and V R M acquired and analysed the flight data. S D E and V R M produced the visualizations. S R H B, S K, F A, R L S and S D E supervised the study. V R M wrote the paper, with inputs from S R H B, S K, F A, R L S and S D E.

## Conflict of interest

The authors declare no competing interests.

## Data and code availability statement

The code and datasets generated and/or analysed during the current study are available from the corresponding author.

## Additional information

Correspondence should be directed towards Steven Barrett (<sup>2</sup>).

## ORCID iDs

Sebastian D Eastham  <https://orcid.org/0000-0002-2476-4801>

Raymond L Speth  <https://orcid.org/0000-0002-8941-4554>

Steven R H Barrett  <https://orcid.org/0000-0002-4642-9545>

## References

- [1] Schumann U 1996 On conditions for contrail formation from aircraft exhausts *Meteorol. Z.* **5** 4–23
- [2] Kärcher B 2018 Formation and radiative forcing of contrail cirrus *Nat. Commun.* **9** 1824
- [3] Spangenberg D A, Minnis P, Bedka S T, Palikonda R, Duda D P and Rose F G 2013 Contrail radiative forcing over the northern hemisphere from 2006 Aqua MODIS data: contrail radiative forcing from MODIS *Geophys. Res. Lett.* **40** 595–600
- [4] Mannstein H, Spichtinger P and Gierens K 2005 A note on how to avoid contrail cirrus *Transp. Res. D* **10** 421–6
- [5] Gierens K, Lim L and Eleftheratos K 2008 A review of various strategies for contrail avoidance *Open Atmos. Sci. J.* **2** 1–7
- [6] Teoh R, Schumann U, Majumdar A and Stettler M E J 2020 Mitigating the climate forcing of aircraft contrails by small-scale diversions and technology adoption *Environ. Sci. Technol.* **54** 2941–50
- [7] Burkhardt U and Kärcher B 2011 Global radiative forcing from contrail cirrus *Nat. Clim. Change* **1** 54–58
- [8] Caiazzo F, Agarwal A, Speth R L and Barrett S R H 2017 Impact of biofuels on contrail warming *Environ. Res. Lett.* **12** 114013
- [9] Bock L and Burkhardt U 2019 Contrail cirrus radiative forcing for future air traffic *Atmos. Chem. Phys.* **19** 8163–74
- [10] Sanz-Morère I, Eastham S D, Speth R L and Barrett S R H 2020 Reducing uncertainty in contrail radiative forcing resulting from uncertainty in ice crystal properties *Environ. Sci. Technol. Lett.* **7** 371–5
- [11] Mannstein H, Meyer R and Wendling P 1999 Operational detection of contrails from NOAA-AVHRR-data *Int. J. Remote Sens.* **20** 1641–60
- [12] Palikonda R, Minnis P, Duda D P and Mannstein H 2005 Contrail coverage derived from 2001 AVHRR data over the continental United States of America and surrounding areas *Meteorol. Z.* **14** 525–36
- [13] Duda D P, Minnis P, Khlopenkov K, Chee T L and Boeke R 2013 Estimation of 2006 northern hemisphere contrail coverage using MODIS data *Geophys. Res. Lett.* **40** 612–7
- [14] Bedka S T, Minnis P, Duda D P, Chee T L and Palikonda R 2013 Properties of linear contrails in the northern hemisphere derived from 2006 Aqua MODIS observations *Geophys. Res. Lett.* **40** 772–7
- [15] Duda D P, Bedka S T, Minnis P, Spangenberg D, Khlopenkov K, Chee T and Smith W L Jr 2019 Northern hemisphere contrail properties derived from Terra and Aqua MODIS data for 2006 and 2012 *Atmos. Chem. Phys.* **19** 5313–30
- [16] Vázquez-Navarro M, Mannstein H and Mayer B 2010 An automatic contrail tracking algorithm *Atmos. Meas. Tech.* **3** 1089–101
- [17] Vázquez-Navarro M, Mannstein H and Kox S 2015 Contrail life cycle and properties from 1 year of MSG/SEVIRI rapid-scan images *Atmos. Chem. Phys.* **15** 8739–49
- [18] Gierens K and Vázquez-Navarro M 2018 Statistical analysis of contrail lifetimes from a satellite perspective *Meteorol. Z.* **27** 88472
- [19] Duda D P, Minnis P, Nguyen L, Palikonda R and Case A 2004 Study of the development of contrail clusters over the great lakes *J. Atmos. Sci.* **61** 1132–46
- [20] Zhang G, Zhang J and Shang J 2018 Contrail recognition with convolutional neural network and contrail parameterizations evaluation *SOLA* **14** 132–7
- [21] Schmit T J, Lindstrom S S, Gerth J J and Gunshor M M (NOAA/NESDIS Center for Satellite Applications and Research Advanced Satellite Products Branch, Madison, Wisconsin) 2018 Applications of the 16 spectral bands on the Advanced Baseline Imager (ABI) *J. Operat. Meteor.* **06** 33–46
- [22] GOES-R Algorithm Working Group & GOES-R Series Program 2017 NOAA GOES-R Series Advanced Baseline



- Imager (ABI) Level 2+ Cloud and Moisture Imagery Products (CMIP) (<https://doi.org/10.7289/V5736P36>)
- [23] Schafer M, Strohmeier M, Lenders V, Martinovic I and Wilhelm M 2014 Bringing up OpenSky: a large-scale ADS-B sensor network for research *IPSN-14 Proc. 13th Int. Symp. on Information Processing in Sensor Networks* (IEEE) pp 83–94
- [24] Minnis P, Kirk Ayers J and Weaver S P 1997 Surface-based observations of contrail occurrence frequency over the US, April 1993–April 1994 *NASA Ref. Publ. 1404* pp 1157–60
- [25] Meyer R, Buell R, Leiter C, Mannstein H, Pechtl S, Oki T and Wendling P 2007 Contrail observations over Southern and Eastern Asia in NOAA/AVHRR data and comparisons to contrail simulations in a GCM *Int. J. Remote Sens.* **28** 2049–69
- [26] Feofilov A G and Stubenrauch C J 2019 Diurnal variation of high-level clouds from the synergy of AIRS and IASI space-borne infrared sounders *Atmos. Chem. Phys.* **19** 13957–72
- [27] Minnis P, Bedka S T, Duda D P, Bedka K M, Chee T, Ayers J K, Palikonda R, Spangenberg D A, Khlopenkov K V and Boeke R 2013 Linear contrail and contrail cirrus properties determined from satellite data: contrail cirrus properties from MODIS *Geophys. Res. Lett.* **40** 3220–6
- [28] Schumann U, Bugliaro L, Dörnbrack A, Baumann R and Voigt C 2021 Aviation contrail cirrus and radiative forcing over Europe during 6 months of COVID-19 *Geophys. Res. Lett.* **48**
- [29] Quaas J, Gryspeerdt E, Vautard R and Boucher O 2021 Climate impact of aircraft-induced cirrus assessed from satellite observations before and during COVID-19 *Environ. Res. Lett.* **16** 064051
- [30] United States Department of Transportation 2021 *US Carrier Traffic Statistics* (available at: [www.transtats.bts.gov/TRAFFIC/](http://www.transtats.bts.gov/TRAFFIC/))
- [31] Gettelman A, Chen -C-C and Bardeen C G 2021 The climate impact of COVID-19-induced contrail changes *Atmos. Chem. Phys.* **21** 9405–16
- [32] Schumann U et al 2021 Air traffic and contrail changes over Europe during COVID-19: a model study *Atmos. Chem. Phys.* **21** 7429–50
- [33] Ronneberger O, Fischer P and Brox T 2015 U-net: convolutional networks for biomedical image segmentation (arXiv:1505.04597 [Cs])
- [34] He K, Zhang X, Ren S and Sun J 2016 Deep residual learning for image recognition *2016 IEEE Conf. on Computer Vision and Pattern Recognition (CVPR)* (IEEE) pp 770–8
- [35] Kingma D P and Ba J 2017 Adam: a method for stochastic optimization (arXiv:1412.6980 [Cs])
- [36] Hersbach H et al ERA5 hourly data on pressure levels from 1979 to present *Copernicus Climate Change Service (C3S) Climate Data Store (CDS)* (<https://doi.org/10.24381/cds.bd0915c6>)